HHS Public Access

Author manuscript

Behav Brain Res. Author manuscript; available in PMC 2024 February 15.

Published in final edited form as:

Behav Brain Res. 2023 February 15; 439: 114221. doi:10.1016/j.bbr.2022.114221.

Motor deficit and lack of overt dystonia in Dlx conditional *Dyt1* knockout mice

David Berryman[1,2], **Jake Barrett**[1], **Canna Liu**[1], **Christian Maugee**[1,2], **Julien Waldbaum**[1], **Daiyao Yi**[3], **Hong Xing**[1], **Fumiaki Yokoi**[1], **Shreya Saxena**[3], **Yuqing Li**[1,2,*]

[1]Norman Fixel Institute for Neurological Diseases, Department of Neurology, College of Medicine, University of Florida, Gainesville, FL

[2]Genetics Institute, University of Florida, Gainesville, FL

[3]Herbert Wertheim College of Engineering, Department of Electrical and Computer Engineering, University of Florida, Gainesville FL

Abstract

DYT1 or DYT-TOR1A dystonia is early-onset generalized dystonia caused by a trinucleotide deletion of GAG in the *TOR1A* or *DYT1* gene leads to the loss of a glutamic acid residue in the resulting torsinA protein. A mouse model with overt dystonia is of unique importance to better understand the DYT1 pathophysiology and evaluate preclinical drug efficacy. DYT1 dystonia is likely a network disorder involving multiple brain regions, particularly the basal ganglia. *Tor1a* conditional knockout in the striatum or cerebral cortex leads to motor deficits, suggesting the importance of corticostriatal connection in the pathogenesis of dystonia. Indeed, corticostriatal long-term depression impairment has been demonstrated in multiple targeted DYT1 mouse models. Pappas and colleagues developed a conditional knockout line (Dlx-CKO) that inactivated *Tor1a* in the forebrain and surprisingly displayed overt dystonia. We set out to validate whether conditional knockout affecting both cortex and striatum would lead to overt dystonia and whether machine learning-based video behavioral analysis could be used to facilitate high throughput preclinical drug screening. We generated Dlx-CKO mice and found no overt dystonia or motor deficits at 4 months. At 8 months, retesting revealed motor deficits in rotarod, beam walking, grip strength, and hyperactivity in the open field; however, no overt dystonia was visually discernible or through the machine learning-based video analysis. Consistent with other targeted DYT1 mouse models, we observed age-dependent deficits in the beam walking test, which is likely a better motor behavioral test for preclinical drug testing but more labor-intensive when overt dystonia is absent.

[*]Corresponding author: Dr. Yuqing Li, Corresponding author's address: Department of Neurology, College of Medicine, University of Florida, PO Box 100236, Gainesville, FL 32610-0236, USA, Corresponding author's phone and fax: Tel.:1-352-273-6546; Fax: 1-352-273-5989, yuqingli@ufl.edu.

Authors Roles

Conceptualization, DB, YL; Investigation, DB, JB, CL, CM, JW, DY, HX, FY, SS, YL.; Formal analysis: DB, CM, DY, SS, YL; Writing - original draft: DB; Writing - review & editing: DB, DY, FY, SS, YL.

Ethical Statement

The authors declare no competing financial interests

Keywords

beam walking; *Dlx-Cre* ; dystonia; DYT1; torsinA; *Tor1a*

1. Introduction

Dystonia is the third most common movement disorder behind Parkinson's disease and the tremor, resulting from the abnormal functioning of the brain, with about 250,000 people afflicted in the United States alone. Of those 250,000, about 16,000 to 24,000 are DYT1 dystonia [1]. DYT1 or DYT-TOR1A dystonia is a type of early-onset generalized dystonia characterized by sustained or intermittent muscle contractions causing abnormal or repetitive movements, postures, or both, most commonly manifesting as abnormal flexion in the knee or foot [2]. DYT1 is caused by a heterozygous in-frame trinucleotide GAG deletion in the 5th exon of the *TOR1A* or *DYT1* gene that leads to the loss of a glutamic acid residue in the resulting torsinA protein [3]. DYT1 dystonia disproportionally affects those of Ashkenazi Jewish heritage due to a founder effect [4]. The mechanism of how mutant torsinA protein leads to disease manifestation is poorly understood. DYT1 dystonia is an autosomal dominant disease with reduced penetrance at about 30%, possibly modulated by interacting genetic factors [5]. TorsinA is a member of the AAA+ (ATPases Associated with diverse cellular Activities) family of proteins [3]. TorsinA level is reduced in both fibroblasts derived from DYT1 patients [6] and *Tor1a* knock-in mouse striatum [7], suggesting that partial loss of torsinA contributes to this disorder, ultimately compromising the cerebellothalamocortical connectivity [8] and synaptic homeostasis [9], disrupting nuclear laminar protein function [6,10], or malfunctioning of interactome or chaperone roles [11,12]. There is currently no cure for DYT1 dystonia therefore all treatments are based on alleviating symptoms. These often have limited effect due to dose-limiting side effects of anticholinergics or are highly invasive, like pallidal deep brain stimulation [13–16].

Historically, dystonia has been attributed to the malfunction of the basal ganglia and its connectivity, reviewed extensively [17–19]. However, more evidence has led to a developing view of dystonia as a network disorder involving multiple brain regions [20]. New attention has recently been paid to the cerebellum's role in pathogenesis [21–24]. It has also been shown that disruption of input from afferent sensory neurons combined with a compromised nigrostriatal pathway can lead to dystonia [25]. This supports the shift from the pathogenesis of dystonia resulting from abnormal functioning of just the basal ganglia to an integrated network disorder, including the compromised connectivity of basal ganglia, cerebellum, and cortical motor areas.

Previous work generating tissue-specific conditional deletion and knock-in mice to manipulate this network-level connectivity can lead to motor deficits but fail to exhibit overt dystonia present in human patients [26–31]. We have demonstrated that *Tor1a* conditional knockout in the striatum or cerebral cortex leads to motor deficits suggesting the importance of corticostriatal connection in the pathogenesis of dystonia [27,29]. The striatum, as the main component of the basal ganglia, is mainly composed of medium spiny neurons and large cholinergic interneurons (LCIs), whose dysregulation plays a critical role in

the pathophysiology of DYT1 dystonia [32–45]. LCIs have been observed to have an autoregulation mechanism characterized by spontaneous firing patterns affected by intrinsic membrane properties rather than synaptic input [46–49]. It has also been observed that acetylcholine or muscarine can reduce cholinergic interneuron firing through muscarinic M2/M4 receptors [50–52]. Interestingly it has recently been observed that a blockade of M4 muscarinic receptors on striatal cholinergic interneurons in DYT1 mouse models normalizes striatal dopamine release [53]. There is also alleviation of motor deficits in beam walking test, rescues in dopamine neurotransmission, and alleviation of reduced corticostriatal LTD through administration of anticholinergics like trihexyphenidyl in the knock-in mice that collectively suggest altered communication between cholinergic interneurons and medium spiny neurons may be involved in motor control abnormalities in targeted DYT1 mouse models [54,55].

High throughput identification of potential DYT1 therapeutics has recently vastly improved. Screening the ability to normalize protein mislocalization of TorsinA ΔGAG in knockin mouse models identified 18 compounds from the NCATS Pharmaceutical Collection, including the HIV protease inhibitor ritonavir, as potentially viable therapeutics [56]. However, to further examine the effects of these potential therapeutics like ritonavir, labor-intensive and time-consuming procedures, including validating their effect in animal models, remains the most popular choice [57]. Determining the most appropriate quantification method for the effect of these treatments on the brain of a dystonic mouse is of paramount importance. Behavioral and motor coordination tests as assays are reductionist in nature and provide a narrow view into an animal's pathology and drug effect [58,59], thus typically requiring supplementation with other forms of analysis. This data collection is a time consuming and error-prone process often prohibitively inefficient in today's data intense world. However, recent advances in machine vision have led to new analysis methods to reduce labor and increase accessibility [60–62]. With this understanding, the application of machine vision to generate a high throughput preclinical drug screening is of value in both increased efficiency and precision. We explored whether the application of DeepLabCut (DLC) markerless pose estimation of user-defined body parts with deep learning [62,63] could quickly identify overt dystonia symptoms in mouse models for use in high throughput preclinical drug screening. We supplemented this investigation with more traditional means of assaying motor abnormalities in murine models like accelerated rotarod, beam walking, open field and grip strength tests to form a complete picture of the model's condition and compare their ability to discern dystonic symptoms.

In this framework of DYT1 dystonia as a network disease, the Dauer group developed a Dlx-CKO mouse that targeted *Tor1a* in progenitors of forebrain cholinergic neurons and GABAergic neurons of the cerebral cortex [41]. This model surprisingly has overt dystonia characterized by abnormal twisting-like movements that coincide with selective degeneration of dorsal striatal LCIs, and LCI abnormalities in electrophysiology and connectivity. Motor deficits in their Dlx-CKO mice were observed through increased limb clasping, decreased performance in the grid-hang test, and robust hyperactivity in open field analysis. We generated Dlx-CKO mice to characterize any abnormal motor behaviors. We set out to investigate whether conditional knockout affecting both cortex and striatum would lead to overt dystonia and whether machine learning-based video behavioral analysis could

be used to diagnose pose abnormalities; or if not, what is the most appropriate test for assaying motor abnormalities in the dystonic mouse.

2. Material and Methods

2.1. Animals

All experiments were approved by the Institutional Animal Care and Use Committee at the University of Florida (Protocols: 202110195, 202009761) in accordance with guidelines for the care and use of laboratory animals. The mice were housed under the condition of 12 h-light and 12 h-dark with ad libitum access to food and water. Dlx5/6Cre animals were obtained from Jackson Lab (Tg(dlx6a-Cre)1Mekk/J; stock number 008199, [64]), and the *Tor1a*^{flx} as well as the *Tor1a*$^{-}$ alleles were generated and maintained in house as previously described in C57BL/6 background as is recommended for mouse behavioral testing [27]. Animals were generated following the breeding scheme *Dlx-Cre*$^{+/-}$ *Tor1a*$^{+/-}$ × *Tor1a*$^{flx/flx}$. The *Dlx-cre* allele was maintained with *Tor1a*$^{+/-}$ to avoid potential germline recombination. All experiments involving Dlx-CKO animals used littermate controls (FloxC and CreC, Fig 1A) to reduce variability further. After it was determined that there was no significant difference in motor performance between CreC and FloxC animals, they were combined as control mice to be analyzed versus the Dlx-CKO mice. The deletion of exons 3 and 4 for *Tor1a*$^{-}$ was genotyped by primer set tcko (fw: 5'-CGGCTGAGCTATGCAGAACTA and rev: 5'-CCATAGCTGGACCTGCAATTAAG) as previously described [27]. The presence of *cre* was confirmed via primers fw: 5'-CAGCTAAACATGCTTCATCGTC and rev:5'-GTTATTCGGATCATCAGCTACACC. *Tor1a*^{flx} sites were confirmed with primers fw:5'-GAGGAGAAAATAGGGGCTCAGTAT and rev: 5'-GAAGGTTGAGAAACTGCCTTAGAG.

2.2. Western Blot

For western blot analysis, 2 male and 2 female each of CKO, CreC, and FloxC age-matched animals were sacrificed to confirm conditional knockout at four months of age (Fig 1B). After animal sacrifice, the striatum was dissected and quickly frozen in liquid nitrogen. The striata were homogenized in 200 ml of ice-cold lysis buffer [50mM Tris-Cl (pH 7.4), 175mM NaCl, 5mM EDTA, Protease inhibitor tablets (Roche Ref: 04693124001)] and sonicated for 30 seconds to generate cell lysates. Triton X-100 was added to cell lysate to a final concentration of 1%, vortexed, and incubated for 30 min on ice. These lysates were centrifuged at 10,000 g for 15 min at 4°C to collect the supernatant. Bradford assay was performed using bovine serum albumin as standard to calculate protein concentration and subsequently standardized to 1μg/μl for loading. The samples were mixed with the SDS-PAGE loading buffer, boiled for 5 min, chilled on ice for 1 min, and then centrifuged for 5 min to obtain the supernatant. 15 μg of the sample was then loaded into 10% Tris-Glycine SDS gels. Separated protein bands were transferred to the Millipore Immobilon-FL transfer polyvinylidene difluoride (PVDF) membrane at 100 V for 1 hour. After blocking, the membrane was incubated overnight at 4°C with mouse primary calnexin antibody (MAB3126: *Chemicon International)* for internal loading control and rabbit primary torsinA antibody (Ab34540: *Abcam)*. The membrane was then incubated with the anti-mouse and anti-rabbit secondary antibodies (*Li*-Cor) for an hour

at room temperature, blocked from light. Membranes were imaged using Odyssey CLx-imager to visualize torsinA and calnexin standard control. Following TorsinA imaging, membranes were stripped using LI-COR stripping buffer. Membranes were re-incubated with antibodies for ChAT (Millipore, AB144P) and VAChT (Millipore, ABN100) and with glyceraldehyde-3-phosphate dehydrogenase (GAPDH) as control (Fig 5). Each protein's molecular weight was estimated by comparing the migration distance of the corresponding protein band with the pre-stained protein standard ladder (Bio-rad, #1610373).

2.3. Tail Suspension Test

The tail suspension test was performed to assess abnormal postural behavior at 4 months of age. After a 1-hour acclimation period in a sound-attenuated testing room, mice were picked up by the tail and suspended in the air for 60 seconds 6 inches above the ground and observed for the presence of forelimb and hindlimb clasping as well as trunk clasping as described by [41]. Recordings of this were used for the application of DeepLabCut Markerless pose estimation software [62], and recordings at 8 months were scored for clasping and abnormal movements by 2 independent investigators blinded to genotypes [41]. 4-month cohort had 31 mice (14 CKO [9 male, 5 female], 9 CreC [6 male, 3 female], 8 FloxC [6 male, 2 female]) at 135.6 ± 18.4 days old; 8-month cohort had 34 mice (17 CKO [12 male, 5 female], 11 CreC [7 male, 4 female], 6 FloxC [5 male, 1 female]) at 257.1 ± 16.4 days old.

2.4. DeepLabCut

We applied DLC pose estimation software [63] to quantify the overt dystonic phenotype present in the tail suspension test recordings in the Dlx-CKO mice compared to their control littermates. We trained the network on 620 frames of video recordings of mice undergoing tail suspension test at 4 months and 380 frames at 8 months (60 seconds apiece at 30 fps with 720x480 resolution on a total of 31 mice at 4 months and 120 fps with 1920x1080 resolution on a total of 19 mice at 8 months). About 20 representative frames were extracted using DLC. A total of 17 body parts were labeled, comprising the hindlimbs and tail-base labeled by an investigator blinded to the animal's genotype. Training of the network was done for 50,000 iterations until loss plateaued. Features for K-means cluster analysis of the labeled videos were chosen to be those reflective of dystonic phenotypes observable in both published work and expectedly present in the Dlx-CKO mice [41,65]: mean distance between hindpaws and the tail-base. For k-means analysis we used Python (*sklearn.cluster.kmeans*)[66] to implement K-means with a random seed for initialization. We implemented this five times and there was no change in results, and we reported one of the random initializations. Additionally, when checking SVM classification, we used Python (*sklearn.svm*) to implement the SVM classifier, with 22 subjects as the training set and the remaining as the testing set. We implemented this five times and shuffled the dataset every time to get different sets of training and testing. The classifier failed to classify the groups. Agreement between clustered videos and true genotype of the animals was used to measure the efficiency of the network to identify dystonic phenotype in Dlx-CKO animals, where agreement is calculated as = (TP + TN) / (TP + TN + FP + FN), where TP = True Positive, TN = True Negative, FP = False Positive, and FN = False Negative. We permute the clusters one (control group) and two (Dlx-CKO) optimally to obtain the maximum accuracy.

2.5. Open Field

The open-field test was performed during the light period, as previously described [35]. After a 1-hour acclimation period in a sound-attenuated testing room, each mouse was placed in the center of a VersaMax Legacy plexiglass open field apparatus connected to a computerized Digiscan System (Accuscan Instruments, Inc. OH) and continuously monitored for 30 minutes at 1 min intervals. The 8-month cohort was tested at 262.1 ± 16.4 days old.

2.6. Accelerated Rotarod

The accelerated rotarod test assesses the ability of mice to maintain balance and coordination on an accelerating rotating rod. After a 1 hour acclimation period to a sound-attenuated testing room, the motor performance of mice was examined with an accelerating rotarod (Ugo Basile) as previously described [35]. The apparatus started at an initial speed of 4 rpm, and then one mouse was put on a slot before the rod speed was gradually accelerated at a rate of 0.2 rpm/s. The latency to fall was measured with a cutoff time of 3 min at a final rate of 40 rpm. Each mouse tested was placed in the same slot to minimize variations. Mice were tested for three trials each day for 2 days. The trials within the same day were performed at about 1-hour intervals to allow time for rest. Mice were tested at around 4 months (124.6 ± 18.4 days) and 8 months (244.1 ± 16.4 days) of age.

2.7. Beam Walking

The beam walking test assesses the coordination and balance of mice as they traverse beams of decreasing width and differing shape. The test was performed after acclimation to a sound-attenuated testing room for a 1-hour period as described previously [35]. Initially, the mice were trained to traverse a medium square beam (14 mm wide) in three consecutive trials each day for 2 days walking from a light source towards a cage containing food. On the third day, after training, the mice were tested for two trials on two separate beams, twice on a medium square beam and twice on a medium round beam (17 mm diameter). On the fourth day, the mice were tested for two trials on two separate beams, twice on a small round beam (10 mm diameter) followed by twice on a small square beam (7 mm wide). The number of hind paw slips on each side was counted by investigators blind to the genotypes. All 4 beams were 100 cm long, and the slips traversing the middle 80 cm were counted. The 4-month cohort was tested at 130.6 ± 18.4 days old, while the 8-month cohort was tested at 251.5 ± 16.4 days old.

2.8. Grip Strength

We used a grip strength meter (BIO-GS3, BIOSEB) to assess forelimb and hind limb strength. The meter records the force of a metal grate being pulled in grams. After a 1-hour acclimation period in a sound-attenuated testing room, mice were measured for the strength of both forelimbs and hindlimbs. An investigator blinded to genotype placed each mouse on the metal grate until they gripped it, and they were then pulled away by their tail, and their strength was recorded. To measure forelimb strength, we loosely held the mice by the skin behind their neck and had them hold onto the grate with just their front limbs before pulling back and recording their strength. Each measurement was recorded for three separate trials.

The maximum of these three trials was used for analysis. The 8-month cohort was tested at 277.5 ± 16.4 days old.

2.9. Statistics

All data were tested for normality using the SAS statistical package. The beam walking data was not normally distributed, and we used generalized estimation equations (SAS GENMOD with GEE) with a negative binomial distribution. Two-way interactions between genotype and age, weight, and sex were explored first. Once it was clear there was no statistical difference between CreC and FloxC controls; they were combined as a control group. The rotarod data were analyzed using SAS PHREG and GENMOD with GEE procedures where mice remaining on the beam at 180 seconds were censored for survival analysis to determine a marginal hazard ratio. When looking at open-field data, any measurement of a discrete distribution was analyzed using a negative binomial, while any continuous distribution involving time was analyzed using a gamma distribution. The grip strength data were not normally distributed. Therefore, GENMOD procedure with gamma distribution was used. Tail suspension scoring by independent investigators was also analyzed using the GENMOD procedure with gamma distribution. Western blots were analyzed using R program glm [67]. A shuffle test was performed to assess DLC's ability to predict genotypes accurately based on the agreement between genotypes ad clusters. Labels "Dlx-CKO" and "Control" were randomly reassigned 100,000 times, the agreement between the K-means clustering and surrogate assignments was calculated each time, and the subsequent distribution of surrogate agreements compared to the true agreement value via a 2-way t-test to assess the probability of calculated agreement arising from chance. Significance was assigned at $p < 0.05$.

3. Results

3.1. No motor deficit in accelerated rotarod or beam walking at 4 months

Animals were generated following the breeding scheme *Dlx-Cre*$^{+/-}$ *Tor1a*$^{+/-}$ × *Tor1a*$^{flx/flx}$, with four possible offspring genotypes: *Tor1a*$^{flx/+}$ (WT), *Tor1a*$^{flx/-}$ (Flox control, FloxC), *Dlx-Cre*$^{+/-}$ *Tor1a*$^{flx/+}$ (Cre control, CreC), and *Dlx-Cre*$^{+/-}$ *Tor1a*$^{flx/-}$ (Dlx-CKO) according to expected Mendelian ratios (Fig 1A). The knock-out of striatal torsinA in Dlx-CKO mice was confirmed by Western blot (Fig 1B). Dlx-CKO mice were born according to the Mendelian ratio (data not shown) and had no overt dystonia in contrast to the previous report [41] or at any point up to 4 months of age. Seizures were observed and previously reported in some Dlx-CKO mice [68] but were not present in the over 46 Dlx-CKO mice we produced. We turned to rotarod and beam walking tests to assess motor deficits. Mice hold or stand on the rotarod with 4 paws and the latency to fall, or the amount of time until the mice fall off of the rod, is an indicator of total motor performance, with decreased latency to fall indicative of motor deficit. At 4 months, the Dlx-CKO did not show any significant difference in accelerated rotarod performance (Fig 2A; p=0.88), in agreement with previous findings [41]. We further analyzed motor coordination using the beam walking test after accelerated rotarod analysis. Neither control nor Dlx-CKO mice slipped enough on either the medium square or medium round beam to accurately analyze, but when looking only at slips on small round and small square beams, there was no significant difference between

control and Dlx-CKO mice (Fig 2C; p=0.61). The mice were given time for recovery, and a tail suspension test was done and video recorded. After consultation with the Dauer Lab about the lack of overt dystonia visually discernable in our mice compared to their own, we turned to the application of DLC markerless pose estimation [62] to attempt to use machine vision to reveal some otherwise unobservable difference in animal posture in the 4-month-old cohort. User-applied markers to hindlimb joints on representative frames were used to train a neural network until loss plateau to track markers through recordings. Relative positions of these markers over time were used as features in a k-means cluster analysis for an unsupervised discovery of clusters distinguishing control mice from Dlx-CKO mice. Clustering then based on the average relative distance between left and right hindlimbs as well as right hind limb and the tail-base showed only a 51.62% agreement between k-means predicted genotypes and true genotypes (Fig 3C). Shuffle test of agreement with randomly assigned labels “Dlx-CKO” and “Control” to k-means cluster points shows no significance in this agreement to accurately predict genotype (Fig S1A; p=0.99). Similar results were obtained using supervised approaches such as Support Vector Machines (SVM). These results are not reflective of any reliable use of these markers as a way to distinguish between control and Dlx-CKO mice or revealing of any overt dystonia or machine vision sensitive pose abnormalities in the model.

3.2. Behavioral testing at 8 months reveals deficits in accelerated rotarod, beam walking, forelimb grip strength, and hyperactivity in open field analysis

It is not uncommon for DYT1 mutant animals to develop motor deficits over time [26–28]. Because of this, we allowed the animals to age for four more months under observation before retesting in behavioral assays at around 8 months. As in the 4-month set of tests, the mice were initially tested on the accelerated rotarod. However, contrary to earlier 4-month findings and previous work in the model, mice had significantly decreased latency to fall (Fig 2A; p = 0.0361). The mice were subsequently tested in performance on the beam walking test following the same sequence of behavioral testing done at 4 months. A significantly increased number of slips was observed in Dlx-CKO mice compared to control mice on all beams (Fig 2B; p = 0.0174) and on just small beams (Fig 2C; p = 0.0092), indicative of motor deficit in the mice at 8 months. Tail suspension test was then performed again, and two independent scorers blinded to animal genotype tracked the duration in seconds of “abnormal posturing, clasping or twisting” as defined in previous work on the model [41]. No significant difference was observed in the duration of abnormal posturing between Dlx-CKO animals and control littermates (Fig 4B; p = 0.733). Following the failure to visually discern any presence of overt dystonia, we turned again to DLC using increased FPS and resolution in hopes of increasing sensitivity. However, once again, clustering based on the average relative distance between left and right hindlimbs vs. distance between right hind limb and the tail-base showed only a 52.63% agreement between k-means predicted genotypes and true genotypes (Fig 3D). Again, the shuffle test of agreement with randomly assigned labels “Dlx-CKO” and “Control” to k-means cluster points shows no significance in this agreement to predict genotype (Fig S1B; p=1.0). This contradicts the reported overt dystonia in the Dlx-CKO mice [41,69,70]. Following the tail suspension test, an open field analysis was performed. In agreement with the highly significant hyperactivity previously observed in the model [41], the Dlx-CKO mice were observed to have significantly

increased total distance traveled ($p = 0.0493$), increased total movement time ($p = 0.0427$), and decreased total rest time ($p = 0.0401$), indicative of hyperactivity in open field testing (Table 1). Because previous work in the model observed a significant reduction in grid hang testing, we also measured the grip strength in the Dlx-CKO mice. Forelimb grip strength was significantly reduced in agreement with previous work on the model (Fig 4A; $p = 0.0028$).

3.3. Significant reduction in ChAT and VAChT

The Dlx-CKO mice show significant reductions in LCI number and associated cholinergic markers [41]. To check the integrity of the cholinergic system following torsinA knockout, we performed Western blot analysis on choline acetyltransferase (ChAT) and vesicular acetylcholine transporter (VAChT) in striatum harvested from 12 mice at 4 months. Dlx-CKO mice were found to have a significant reduction in striatal ChAT [ChAT/GAPDH; CT: 0.36 ± 0.03; Dlx-CKO: 0.22 ± 0.03; $p = 0.0037$, Fig 5A, n=6 each] as well as VAChT [VAChT /GAPDH; CT: 0.17 ± 0.01; Dlx-CKO: 0.12 ± 0.02; $p = 0.0149$, Fig 5B, n=6 each], ultimately in agreement with previous work in the model.

4. Discussion

In this study, we set out to determine the practicality of using machine vision for high throughput preclinical drug screening and whether conditional knockout affecting both cortex and striatum would lead to overt dystonia through the use of Dlx-CKO mice, previously characterized by the Dauer group and observed to have overt dystonia. However, we failed to observe overt dystonia in our Dlx-CKO mice at four and eight months. Like most of the targeted DYT1 dystonia mouse models, motor deficits developed at an older age and are observable in the motor tests we performed at 8 months.

We did not observe overt dystonia or dystonic-like movements in the Dlx-CKO mice. We turned to the use of DeepLabCut marker-less pose estimation. Machine vision with deep learning on user-marked body parts offers the potential to reveal differences in posture between our control and Dlx-CKO mice with higher sensitivity than could otherwise be achieved. Ultimately no differences were found. At the 8-month time point following scoring by investigators blinded to genotype, no differences in the duration of abnormal movements were observed despite the development of other motor deficits, nor was DLC able to detect any overt dystonia. This rendered our initial goal of developing a method of high throughput preclinical drug screening based on machine vision pose analysis impossible in the absence of pose differences during the tail suspension.

Several differences in our Dlx-CKO mice compared to those produced by the Dauer lab could potentially impact the manifestation of overt dystonia. One difference between our Dlx-CKO mice and the earlier Dlx-CKO mice generated by the Dauer lab is the location of the loxP sites in the *Tor1a* gene. Cre-mediated recombination removes the 3rd and 4th exons in our line, whereas the 3rd to 5th exons are removed in the other line. Additionally, there could be differences in the microbiomes of the animals, leading to behavioral differences. It has been well established that microbial colonization affects host physiology and can lead to differences in motor performance tests [71–74]. Mouse colony maintenance in

two different facilities can lead to changes in the animal microbiome that, in turn, affect neuronal circuitry and motor performance. Administration of acidified drinking water for *Pseudomonas* control can differentially change a mouse's microbiome and profoundly affect behavioral performance [72,75]. In that same vein, the University of Texas Southwestern animal care facility uses chlorinated reverse osmosis (RO) water to control for a biofilm in the system that could potentially lead to differences in microbiomes between mice we produced given non-chlorinated RO water. It is perhaps a result of these differences in model design and animal care that lead to differences in the presence of overt dystonia, as well as the presence of seizures in a subset of the Dauer group mice [68], something we do not observe in the current study. Additionally, the mice used in this study were of C57BL/6 background, and while the Dauer group did not specify the background of mice used, it has been previously reported that strain specific genetic modifiers can have an effect on behavioral phenotype [76]. It is also possible that greater exploration and understanding of the differences in the results reported here and those reported by the Dauer group yield insight into the mechanisms of penetrance in human DYT1 dystonia.

Dlx-CKO mice performed worse on accelerated rotarod and beam-walking tests, measures of fine motor coordination and balance, as is consistently observed in other targeted DYT1 mouse models [26–28,77–80]. Rotarod and beam walking have been consistently shown to be reliable tests of rodent motor coordination [81–83]. They test the animals in slightly different ways, one of the more obvious differences being accelerated rotarod tests all four limbs while beam walking analysis assays only hindlimb slips. However, it has been established in previous studies that a mere 30% receptor occupancy of GABA-A receptors by benzodiazepine agonists is sufficient to elicit motor performance deficit in beam walking, whereas 70% occupancy was needed in order to observe deficit in accelerated rotarod [84]. Beam walking has also been shown to be one of the most appropriate measures of preclinical drug effect on dystonia in previous studies [54,85]. This supports the use of beam walking as a highly sensitive test for detecting motor deficits in mice.

In addition to beam walking and accelerated rotarod deficits, Dlx-CKO mice also performed worse on forelimb grip strength tests at 8 months, consistent with previous work that showed an inability to hang from a wire grid, a different measure of grip strength. Additionally, mice were observed to be hyperactive in open field analysis, once again in agreement with previous findings. These mice were also previously observed to have degeneration of dorsal striatal LCIs and reduction of associated cholinergic markers. Western blot analysis of our line also finds significantly decreased striatal ChAT and VAChT expression. This implies a conserved cholinergic impairment in both Dlx-CKO models coinciding with the observed motor deficits, supporting a central role of striatal LCIs in the pathogenesis of DYT1 dystonia [17,32–45]. However, our Western blot analysis was conducted at four months of age before the onset of the motor deficits, suggesting factors other than striatal cholinergic impairment might be involved in the development of motor deficits at 8 months we reported here.

Finally, we found Dlx-CKO mice in our hand did not display overt dystonia observable by the naked eye or visible with a machine learning aid. Instead, they have age-dependent motor deficits consistent with other targeted DYT1 models that are observable through

motor coordination tests that likely remain the most appropriate test in preclinical drug screening for DYT1 dystonia in mouse models that lack overt dystonia, but are more labor-intensive.

Supplementary Material

Refer to Web version on PubMed Central for supplementary material.

Acknowledgments

We thank the University of Florida Animal Care Services staff for their help in animal care, Julianne Morrill, Emily Lobosco, Noosha Assary, Pallavi Girdhar, Kaitlyn Brkaric and Katie Grissett, for their technical assistance. We also would like to thank Dr. Zhihua Jiang's lab for using their western blot imager and Dr. Samuel Pappas and Dr. William Dauer for their help in analyzing initial tail suspension recordings for the presence of overt dystonia in mouse development.

Funding

This study was supported by Tyler's Hope for a Dystonia Cure, Inc., National Institutes of Health (grants NS75012, NS111498, NS118397, and NS129873), and the Department of Defense (W81XWH1810099 and W81XWH2110198). FY and YL were partially supported by the Office of the Assistant Secretary of Defense for Health Affairs through the Peer-Reviewed Medical Research Program Discovery Award. Opinions, interpretations, conclusions, and recommendations are those of the author and are not necessarily endorsed by the Department of Defense.

Abbreviations:

LCI	Large cholinergic interneuron
LTD	Long-term depression
DLC	DeepLabCut
NCATS	National Center for Advancing Translational Science
CKO	Conditional knockout
SDS-PAGE	Sodium dodecyl sulfate–polyacrylamide gel electrophoresis
ChAT	Choline acetyltransferase
VAChT	Vesicular acetylcholine transporter
GAPDH	Glyceraldehyde-3-phosphate dehydrogenase

References

[1]. Ozelius LJ, Lubarr N, DYT1 Early-Onset Isolated Dystonia, GeneReviews. (2016) 1–19.

[2]. Albanese A, Bhatia K, Bressman SB, Delong MR, Fahn S, Fung VSC, Hallett M, Jankovic J, Jinnah HA, Klein C, Lang AE, Mink JW, Teller JK, Phenomenology and Classification of dystonia: A Consensus Update, Mov. Disord 28 (2013) 863–873. 10.1002/mds.25475. [PubMed: 23649720]

[3]. Ozelius LJ, Hewett JW, Page CE, Bressman SB, Kramer PL, Shalish C, De Leon D, Brin MF, Raymond D, Corey DP, Fahn S, Risch NJ, Buckler AJ, Gusella JF, Breakefield XO, The early-onset torsion dystonia gene (DYT1) encodes an ATP-binding protein, Nat. Genet 17 (1997) 40–48. 10.1038/ng0997-40. [PubMed: 9288096]

[4]. Bressman SB, Sabatti C, Raymond D, De Leon D, Klein C, Kramer PL, Brin MF, Fahn S, Breakefield X, Ozelius LJ, Risch NJ, The DYT1 phenotype and guidelines for diagnostic testing, Neurology. 54 (2000) 1746–1752. 10.1212/wnl.54.9.1746. [PubMed: 10802779]

[5]. Risch NJ, Bressman SB, Senthil G, Ozelius LJ, Intragenic Cis and Trans Modification of Genetic Susceptibility in DYT1 Torsion Dystonia, Am. J. Hum. Genet 80 (2007) 1188–1193. 10.1086/518427. [PubMed: 17503336]

[6]. Goodchild RE, Kim CE, Dauer WT, Loss of the Dystonia-Associated Protein TorsinA Selectively Disrupts the Neuronal Nuclear Envelope, Neuron. 48 (2005) 923–932. 10.1016/j.neuron.2005.11.010. [PubMed: 16364897]

[7]. Yokoi F, Yang G, Li J, Deandrade MP, Zhou T, Li Y, Earlier onset of motor deficits in mice with double mutations in Dyt1 and Sgce, J. Biochem 148 (2010) 459–466. 10.1093/jb/mvq078. [PubMed: 20627944]

[8]. Argyelan M, Carbon M, Niethammer M, Uluğ AM, Voss HU, Bressman SB, Dhawan V, Eidelberg D, Cerebellothalamocortical Connectivity Regulates Penetrance in Dystonia, J. Neurosci 29 (2009) 9740–9747. 10.1523/JNEUROSCI.2300-09.2009. [PubMed: 19657027]

[9]. Ponterio G, Faustini G, El Atiallah I, Sciamanna G, Meringolo M, Tassone A, Imbriani P, Cerri S, Alpha-Synuclein is Involved in DYT1 Dystonia Striatal Synaptic Dysfunction, 37 (2022) 949–961. 10.1002/mds.29024.

[10]. Ding B, Novel insights into the pathogenesis of DYT1 dystonia from induced patient-derived neurons, Neural Regen. Res 17 (2022) 561–562. 10.4103/1673-5374.320978. [PubMed: 34380890]

[11]. Chase AR, Laudermilch E, Schlieker C, Torsin ATPases: Harnessing Dynamic Instability for Function, Front. Mol. Biosci 4 (2017) 29. 10.3389/fmolb.2017.00029. [PubMed: 28553638]

[12]. Burdette AJ, Churchill PF, Caldwell GA, Caldwell KA, The early-onset torsion dystonia-associated protein, torsinA, displays molecular chaperone activity in vitro, Cell Stress Chaperones. 15 (2010) 605–617. 10.1007/s12192-010-0173-2. [PubMed: 20169475]

[13]. Vidailhet M, Jutras MF, Grabli D, Roze E, Deep brain stimulation for dystonia, J. Neurol. Neurosurg. Psychiatry 84 (2013) 1029–1042. 10.1136/jnnp-2011-301714. [PubMed: 23154125]

[14]. Thenganatt MA, Jankovic J, Treatment of Dystonia, Neurotherapeutics. 11 (2014) 139–152. 10.1007/s13311-013-0231-4. [PubMed: 24142590]

[15]. Jinnah HA, Factor SA, Diagnosis and Treatment of Dystonia, Neurol. Clin 33 (2015) 77–100. 10.1016/J.NCL.2014.09.002. [PubMed: 25432724]

[16]. Balint B, Bhatia KP, Dystonia: An update on phenomenology, classification, pathogenesis and treatment, Curr. Opin. Neurol 27 (2014) 468–476. 10.1097/WCO.0000000000000114. [PubMed: 24978640]

[17]. Breakefield XO, Blood AJ, Li Y, Hallett M, Hanson PI, Standaert DG, The pathophysiological basis of dystonias, Nat. Rev. Neurosci 9 (2008) 222–234. 10.1038/nrn2337. [PubMed: 18285800]

[18]. Peterson DA, Sejnowski TJ, Poizner H, Convergent evidence for abnormal striatal synaptic plasticity in dystonia, Neurobiol. Dis 37 (2010) 558–573. 10.1016/j.nbd.2009.12.003. [PubMed: 20005952]

[19]. Berardelli A, Rothwell JC, Hallett M, Thompson PD, Manfredi M, Marsden CD, The pathophysiology of primary dystonia, Brain. 121 (1998) 1195–1212. 10.1093/brain/121.7.1195. [PubMed: 9679773]

[20]. Prudente CN, Hess EJ, Jinnah HA, Dystonia as a Network Disorder : What is the Role of the Cerebellum?, Neuroscience. 260 (2014) 23–35. 10.1016/j.neuroscience.2013.11.062.Dystonia. [PubMed: 24333801]

[21]. Shakkottai VG, Batla A, Bhatia K, Dauer WT, Dresel C, Niethammer M, Eidelberg D, Raike RS, Smith Y, Jinnah HA, Hess EJ, Meunier S, Hallett M, Fremont R, Khodakhah K, LeDoux MS, Popa T, Gallea C, Lehericy S, Bostan AC, Strick PL, Current Opinions and Areas of Consensus on the Role of the Cerebellum in Dystonia, Cerebellum 16 (2017) 577–594. 10.1007/s12311-016-0825-6. [PubMed: 27734238]

[22]. Avanzino L, Abbruzzese G, How does the cerebellum contribute to the pathophysiology of dystonia?, Basal Ganglia. 2 (2012) 231–235. 10.1016/j.baga.2012.05.003.

[23]. Sadnicka A, Hoffland BS, Bhatia KP, van de Warrenburg BP, Edwards MJ, The cerebellum in dystonia - Help or hindrance?, Clin. Neurophysiol 123 (2012) 65–70. 10.1016/j.clinph.2011.04.027. [PubMed: 22078259]

[24]. Filip P, Lungu OV, Bareš M, Dystonia and the cerebellum: A new field of interest in movement disorders?, Clin. Neurophysiol 124 (2013) 1269–1276. 10.1016/j.clinph.2013.01.003. [PubMed: 23422326]

[25]. Schicatano EJ, Basso MA, Evinger C, Animal Model Explains the Origins of the Cranial Dystonia Benign Essential Blepharospasm, J. Neurophysiol 77 (1997) 2842–2846. 10.1152/jn.1997.77.5.2842. [PubMed: 9163399]

[26]. Dang MT, Yokoi F, McNaught KSP, Jengelley TA, Jackson T, Li J, Li Y, Generation and characterization of Dyt1 ΔgAG knock-in mouse as a model for early-onset dystonia, Exp. Neurol 196 (2005) 452–463. 10.1016/j.expneurol.2005.08.025. [PubMed: 16242683]

[27]. Yokoi F, Dang MT, Mitsui S, Li J, Li Y, Motor Deficits and Hyperactivity in Cerebral Cortex-specific Dyt1 Conditional Knockout Mice, J. Biochem 143 (2008) 39–47. 10.1093/jb/mvm191. [PubMed: 17956903]

[28]. Yokoi F, Dang MT, Li Y, Improved motor performance in Dyt1 ΔGAG heterozygous knock-in mice by cerebellar Purkinje-cell specific Dyt1 conditional knocking-out, Behav. Brain Res 230 (2012) 389–398. 10.1016/j.bbr.2012.02.029. [PubMed: 22391119]

[29]. Yokoi F, Dang MT, Li J, Standaert DG, Li Y, Motor Deficits and Decreased Striatal Dopamine Receptor 2 Binding Activity in the Striatum-Specific Dyt1 Conditional Knockout Mice, PLoS One. 6 (2011). 10.1371/journal.pone.0024539.

[30]. Oleas J, Yokoi F, Deandrade MP, Pisani A, Li Y, Engineering animal models of dystonia, Mov. Disord 28 (2013) 990–1000. 10.1002/mds.25583. [PubMed: 23893455]

[31]. Weisheit CE, Dauer WT, A novel conditional knock-in approach defines molecular and circuit effects of the DYT1 dystonia mutation, Hum. Mol. Genet 24 (2015) 6459–6472. 10.1093/hmg/ddv355. [PubMed: 26370418]

[32]. Eskow Jaunarajs KL, Scarduzio M, Ehrlich ME, McMahon LL, Standaert DG, Diverse Mechanisms Lead to Common Dysfunction of Striatal Cholinergic Interneurons in Distinct Genetic Mouse Models of Dystonia, J. Neurosci 39 (2019) 7195–7205. 10.1523/JNEUROSCI.0407-19.2019. [PubMed: 31320448]

[33]. Eskow Jaunarajs KL, Bonsi P, Chesselet MF, Standaert DG, Pisani A, Striatal cholinergic dysfunction as a unifying theme in the pathophysiology of dystonia, Prog. Neurobiol 127-128 (2015) 91–107. 10.1016/j.pneurobio.2015.02.002. [PubMed: 25697043]

[34]. Liu Y, Xing H, Yokoi F, Vaillancourt DE, Li Y, Investigating the role of striatal dopamine receptor 2 in motor coordination and balance: Insights into the pathogenesis of DYT1 dystonia, Behav. Brain Res 403 (2021) 113137. 10.1016/j.bbr.2021.113137. [PubMed: 33476687]

[35]. Liu Y, Xing H, Sheng W, Singh KN, Korkmaz AG, Comeau C, Anika M, Ernst A, Yokoi F, Vaillancourt DE, Frazier CJ, Li Y, Alteration of the cholinergic system and motor deficits in cholinergic neuron-specific Dyt1 knockout mice, Neurobiol. Dis 154 (2021) 105342. 10.1016/j.nbd.2021.105342. [PubMed: 33757902]

[36]. Wilkes BJ, DeSimone JC, Liu Y, Chu WT, Coombes S, Li Y, Vaillancourt DE, Cell-specific effects of Dyt1 knock-out on sensory processing, network-level connectivity, and motor deficits, Exp. Neurol (2021) 113783. 10.1016/j.expneurol.2021.113783. [PubMed: 34119482]

[37]. Pisani A, Bernardi G, Ding J, Surmeier DJ, Re-emergence of striatal cholinergic interneurons in movement disorders, Trends Neurosci. 30 (2007) 545–553. 10.1016/j.tins.2007.07.008. [PubMed: 17904652]

[38]. Martella G, Tassone A, Sciamanna G, Platania P, Cuomo D, Viscomi MT, Bonsi P, Cacci E, Biagioni S, Usiello A, Bernardi G, Sharma N, Standaert DG, Pisani A, Impairment of bidirectional synaptic plasticity in the striatum of a mouse model of DYT1 dystonia: Role of endogenous acetylcholine, Brain. 132 (2009) 2336–2349. 10.1093/brain/awp194. [PubMed: 19641103]

[39]. Sciamanna G, Tassone A, Mandolesi G, Puglisi F, Ponterio G, Martella G, Madeo G, Bernardi G, Standaert DG, Bonsi P, Pisani A, Cholinergic dysfunction alters synaptic integration between

thalamostriatal and corticostriatal inputs in DYT1 dystonia, J. Neurosci 32 (2012) 11991–12004. 10.1523/JNEUROSCI.0041-12.2012. [PubMed: 22933784]

[40]. Sciamanna G, Hollis R, Ball C, Martella G, Tassone A, Marshall A, Parsons D, Li X, Yokoi F, Zhang L, Li Y, Pisani A, Standaert DG, Cholinergic dysregulation produced by selective inactivation of the dystonia-associated protein torsinA, Neurobiol. Dis 47 (2012) 416–427. 10.1016/j.nbd.2012.04.015. [PubMed: 22579992]

[41]. Pappas SS, Darr K, Holley SM, Cepeda C, Mabrouk OS, Wong J-MT, Lewitt TM, Paudel R, Houlden H, Kennedy RT, Levine MS, Dauer WT, Forebrain deletion of the dystonia protein torsinA causes dystonic-like movements and loss of striatal cholinergic neurons, Elife. (2015). 10.7554/eLife.08352.001.

[42]. Pappas SS, Li J, LeWitt TM, Kim JK, Monani UR, Dauer WT, A cell autonomous torsina requirement for cholinergic neuron survival and motor control, Elife. 7 (2018) 1–15. 10.7554/eLife.36691.

[43]. Ponterio G, Tassone A, Sciamanna G, Vanni V, Meringolo M, Santoro M, Mercuri NB, Bonsi P, Pisani A, Enhanced mu opioid receptor–dependent opioidergic modulation of striatal cholinergic transmission in DYT1 dystonia, Mov. Disord 33 (2018) 310–320. 10.1002/mds.27212. [PubMed: 29150865]

[44]. Richter F, Bauer A, Perl S, Schulz A, Richter A, Optogenetic augmentation of the hypercholinergic endophenotype in DYT1 knock-in mice induced erratic hyperactive movements but not dystonia, EBioMedicine. 41 (2019) 649–658. 10.1016/j.ebiom.2019.02.042. [PubMed: 30819512]

[45]. Yokoi F, Oleas J, Xing H, Liu Y, Dexter KM, Misztal C, Gerard M, Efimenko I, Lynch P, Villanueva M, Alsina R, Decreased number of striatal cholinergic interneurons and motor deficits in dopamine receptor 2-expressing-cell-specific Dyt1 conditional knockout mice, Neurobiol. Dis 134 (2020) 104638. 10.1016/j.nbd.2019.104638. [PubMed: 31618684]

[46]. Goldberg JA, Teagarden MA, Foehring RC, Wilson CJ, Nonequilibrium Calcium Dynamics Regulate the Autonomous Firing Pattern of Rat Striatal Cholinergic Interneurons, J. Neurosci 29 (2009) 8396–8407. 10.1523/JNEUROSCI.5582-08.2009. [PubMed: 19571130]

[47]. Goldberg JA, Wilson CJ, Control of Spontaneous Firing Patterns by the Selective Coupling of Calcium Currents to Calcium-Activated Potassium Currents in Striatal Cholinergic Interneurons, J. Neurosci 25 (2005) 10230–10238. 10.1523/JNEUROSCI.2734-05.2005. [PubMed: 16267230]

[48]. Bennett BD, Callaway JC, Wilson CJ, Intrinsic Membrane Properties Underlying Spontaneous Tonic Firing in Neostriatal Cholinergic Interneurons, Neurosci. Res 20 (2000) 8493–8503.

[49]. Wilson CJ, The mechanism of intrinsic amplification of hyperpolarizations and spontaneous bursting in striatal cholinergic interneurons, Neuron. 45 (2005) 575–585. 10.1016/j.neuron.2004.12.053. [PubMed: 15721243]

[50]. Ding J, Guzman JN, Tkatch T, Chen S, Goldberg JA, Ebert PJ, Levitt P, Wilson CJ, Hamm HE, Surmeier DJ, RGS4-dependent attenuation of M4 autoreceptor function in striatal cholinergic interneurons following dopamine depletion, Nat. Neurosci 9 (2006) 832–842. 10.1038/nn1700. [PubMed: 16699510]

[51]. Howe AR, Surmeier DJ, Muscarinic receptors modulate N-, P-, and L-type Ca2+ currents in rat striatal neurons through parallel pathways, J. Neurosci 15 (1995) 458–469. 10.1523/jneurosci.15-01-00458.1995. [PubMed: 7823150]

[52]. Yan Z, Surmeier DJ, Muscarinic (m2/m4) receptors reduce N- and P-type Ca2+ currents in rat neostriatal cholinergic interneurons through a fast, membrane-delimited, G-protein pathway, J. Neurosci 16 (1996) 2592–2604. 10.1523/jneurosci.16-08-02592.1996. [PubMed: 8786435]

[53]. Downs AM, Donsante Y, Jinnah HA, Hess EJ, Blockade of M4 muscarinic receptors on striatal cholinergic interneurons normalizes striatal dopamine release in a mouse model of TOR1A dystonia, Neurobiol. Dis 168 (2022) 105699. 10.1016/j.nbd.2022.105699. [PubMed: 35314320]

[54]. Dang MT, Yokoi F, Cheetham CC, Lu J, Vo V, Lovinger DM, Li Y, An anticholinergic reverses motor control and corticostriatal LTD deficits in Dyt1 ΔGAG knock-in mice, Behav. Brain Res 226 (2012) 465–472. 10.1016/j.bbr.2011.10.002. [PubMed: 21995941]

[55]. Downs AM, Fan X, Donsante C, Jinnah HA, Hess EJ, Trihexyphenidyl rescues the deficit in dopamine neurotransmission in a mouse model of DYT1 dystonia, Neurobiol. Dis 125 (2019) 115–122. 10.1016/j.nbd.2019.01.012. [PubMed: 30707939]

[56]. Caffall ZF, Wilkes BJ, Hernandez-Martinez R, Rittiner JE, Fox JT, Wan KK, Shipman MK, Titus SA, Zhang Y-QQ, Patnaik S, Hall MD, Boxer MB, Shen M, Li Z, Vaillancourt DE, Calakos N, Hernández-Martinez R, Rittiner JE, Fox JT, Wan KK, Shipman MK, Titus SA, Zhang Y-QQ, Patnaik S, Hall MD, Boxer MB, Shen M, Li Z, Vaillancourt DE, Calakos N, The HIV protease inhibitor, ritonavir, corrects diverse brain phenotypes across development in mouse model of DYT-TOR1A dystonia, Sci. Transl. Med 13 (2021) 1–14. 10.1126/scitranslmed.abd3904.

[57]. Haynes EM, Ulland TK, Eliceiri KW, A Model of Discovery: The Role of Imaging Established and Emerging Non-mammalian Models in Neuroscience, Front. Mol. Neurosci 15 (2022) 1–22. 10.3389/fnmol.2022.867010.

[58]. Krakauer JW, Ghazanfar AA, Gomez-Marin A, MacIver MA, Poeppel D, Neuroscience Needs Behavior: Correcting a Reductionist Bias, Neuron. 93 (2017) 480–490. 10.1016/j.neuron.2016.12.041. [PubMed: 28182904]

[59]. Gomez-Marin A, Paton JJ, Kampff AR, Costa RM, Mainen ZF, Big behavioral data: Psychology, ethology and the foundations of neuroscience, Nat. Neurosci 17 (2014) 1455–1462. 10.1038/nn.3812. [PubMed: 25349912]

[60]. Anderson DJ, Perona P, Toward a science of computational ethology, Neuron. 84 (2014) 18–31. 10.1016/j.neuron.2014.09.005. [PubMed: 25277452]

[61]. Dell AI, Bender JA, Branson K, Couzin ID, de Polavieja GG, Noldus LPJJ, Pérez-Escudero A, Perona P, Straw AD, Wikelski M, Brose U, Automated image-based tracking and its application in ecology, Trends Ecol. Evol 29 (2014) 417–428. 10.1016/j.tree.2014.05.004. [PubMed: 24908439]

[62]. Mathis A, Mamidanna P, Cury K, Abe T, Murthy V, Mathis MW, Bethge M, DeepLabCut: markerless pose estimation of user-defined body parts with deep learning, Nat. Neurosci Vol 21 (2018) 1281–1289. 10.1038/s41593-018-0209-y. [PubMed: 30127430]

[63]. Nath T, Mathis A, Chen AC, Patel A, Bethge M, Mathis MW, Using DeepLabCut for 3D markerless pose estimation across species and behaviors, Nat. Protoc 14 (2019) 2152–2176. 10.1038/s41596-019-0176-0. [PubMed: 31227823]

[64]. Monory K, Massa F, Egertová M, Eder M, Westenbroek R, Kelsch W, Jacob W, Marsch R, Long J, Rubenstein JL, Goebbels S, Nave K, Klugmann M, Wölfel B, Dodt H, Wotjak CT, Mackie K, Elphick MR, The Endocannabinoid System Controls Key Epileptogenic Circuits in the Hippocampus, Neuron. 51 (2006) 455–466. [PubMed: 16908411]

[65]. Knorr S, Rauschenberger L, Pasos UR, Friedrich MU, Peach RL, Grundmann-Hauser K, Ott T, O'Leary A, Reif A, Tovote P, Volkmann J, Ip CW, The evolution of dystonia-like movements in TOR1A rats after transient nerve injury is accompanied by dopaminergic dysregulation and abnormal oscillatory activity of a central motor network, Neurobiol. Dis 154 (2021) 105337. 10.1016/j.nbd.2021.105337. [PubMed: 33753289]

[66]. Pedregosa et al., Scikit-learn: Machine Learning in Python, (2011) 2825–2830. https://scikit-learn.org/stable/about.html#citing-scikit-learn.

[67]. R TEAM, R: A language and environment for statistical computing, (2022). https://www.r-project.org/.

[68]. Kernodle K, Bakerian AM, Cropsey A, Dauer WT, Leventhal DK, A dystonia mouse model with motor and sequencing deficits paralleling human disease, Behav. Brain Res 426 (2022) 113844. 10.1016/j.bbr.2022.113844. [PubMed: 35304183]

[69]. DeSimone JC, Pappas SS, Febo M, Burciu RG, Shukla P, Colon-Perez LM, Dauer WT, Vaillancourt DE, Forebrain knock-out of torsinA reduces striatal free-water and impairs whole-brain functional connectivity in a symptomatic mouse model of DYT1 dystonia, Neurobiol. Dis 106 (2017) 124–132. 10.1016/j.nbd.2017.06.015. [PubMed: 28673740]

[70]. Li J, Levin DS, Kim AJ, Pappas SS, Dauer WT, TorsinA restoration in a mouse model identifies a critical therapeutic window for DYT1 dystonia, J. Clin. Invest 131 (2021). 10.1172/JCI139606.

[71]. Heijtz RD, Wang S, Anuar F, Qian Y, Björkholm B, Samuelsson A, Hibberd ML, Forssberg H, Pettersson S, Normal gut microbiota modulates brain development and behavior, Proc. Natl. Acad. Sci. U. S. A 108 (2011) 3047–3052. 10.1073/pnas.1010529108. [PubMed: 21282636]

[72]. Johnson TB, Langin LM, Zhao J, Weimer JM, Pearce DA, Kovács AD, Changes in motor behavior, neuropathology, and gut microbiota of a Batten disease mouse model following administration of acidified drinking water, Sci. Rep 9 (2019) 1–16. 10.1038/s41598-019-51488-z. [PubMed: 30626917]

[73]. Sampson T, Debelius J, Thron T, Janssen S, Shastri G, Ilhan ZE, Challis C, Schretter C, Rocha S, Gradinaru V, Chesselet M-F, Keshavarzian A, Shannon K, Krajmalnik-Brown R, Wittung-Stafshede P, Knight R, Mazmanian S, Gut Microbiota Regulate Motor Deficits and Neuroinflammation in a Model of Parkinson's Disease, Cell. (2017) 1469–1480. 10.2174/1568026615101503282234 28.

[74]. Fisher EMC, Bannerman DM, Mouse models of neurodegeneration: Know your question, know your mouse, Sci. Transl. Med 11 (2019) 1–16. 10.1126/scitranslmed.aaq1818.

[75]. Whipple B, Agar J, Zhao J, Pearce DA, Kovács AD, The acidified drinking water-induced changes in the behavior and gut microbiota of wild-type mice depend on the acidification mode, Sci. Rep 11 (2021) 1–15. 10.1038/s41598-021-82570-0. [PubMed: 33414495]

[76]. Tanabe LM, Martin C, Dauer WT, Genetic background modulates the phenotype of a mouse model of dyt1 dystonia, PLoS One. 7 (2012) 1–9. 10.1371/journal.pone.0032245.

[77]. Grundmann K, Glöckle N, Martella G, Sciamanna G, Hauser T, Yu L, Castaneda S, Pichler B, Fehrenbacher B, Schaller M, Nuscher B, Haass C, Hettich J, Yue Z, Phuc H, Pisani A, Riess O, Ott T, Neurobiology of Disease Generation of a novel rodent model for DYT1 dystonia, Neurobiol. Dis 47 (2012) 61–74. 10.1016/j.nbd.2012.03.024. [PubMed: 22472189]

[78]. Grundmann K, Reischmann B, Vanhoutte G, Hübener J, Teismann P, Hauser T, Bonin M, Wilbertz J, Horn S, Nguyen HP, Kuhn M, Chanarat S, Wolburg H, Van Der Linden A, Riess O, Overexpression of human wildtype torsinA and human Δ GAG torsinA in a transgenic mouse model causes phenotypic abnormalities, Neurobiol. Dis 27 (2020) 190–206. 10.1016/j.nbd.2007.04.015.

[79]. Page ME, Bao L, Andre P, Pelta-heller J, Sluzas E, Gonzalez-alegre P, Bogush A, Khan LE, Iacovitti L, Rice ME, Ehrlich ME, Cell-autonomous alteration of dopaminergic transmission by wild type and mutant (Δ E) TorsinA in transgenic mice, Neurobiol. Dis 39 (2010) 318–326. 10.1016/j.nbd.2010.04.016. [PubMed: 20460154]

[80]. Song C, Fan X, Exeter C, Hess EJ, Jinnah HA, Functional Analysis of Dopaminergic Systems in a DYT1 Knock- in Mouse Model of Dystonia, Neurobiol. Dis 48 (2012) 66–78. 10.1016/j.nbd.2012.05.009.Functional. [PubMed: 22659308]

[81]. Luong TN, Carlisle HJ, Southwell A, Patterson PH, Assessment of motor balance and coordination in mice using the balance beam, J. Vis. Exp (2011) 5–7. 10.3791/2376.

[82]. Carter RJ, Morton J, Dunnett SB, Motor Coordination and Balance in Rodents, Curr. Protoc. Neurosci 15 (2001). 10.1002/0471142301.ns0812s15.

[83]. Buccafusco JJ, Methods of Behavior Analysis in Neuroscience., 2nd ed., CRC Press Taylor and Francis, Boca Raton (FL), USA, 2009.

[84]. Stanley JL, Lincoln RJ, Brown TA, Mcdonald LM, Dawson GR, Reynolds DS, The mouse beam walking assay offers improved sensitivity over the mouse rotarod in determining motor coordination deficits induced by benzodiazepines, J. Psychopharmacol 19 (2005) 221–227. [PubMed: 15888506]

[85]. Cao S, Hewett J, Yokoi F, Lu J, Buckley AC, Burdette A, Chen P, Nery F, Li Y, Breakfield X, Caldwell G, Caldwell K, Chemical enhancement of torsinA function in cell andanimal models of torsion dystonia, Dis. Model. Mech (2010). 10.1242/dmm.003715.

Highlights

1. Lack of overt dystonia and seizure in Dlx-CKO mice made from another floxed line.
2. Negative finding of DeepLabCuts markerless pose estimation applied to Dlx-CKO mice
3. Age-dependent deficit in beam walking, rotarod, grip strength and open field tests
4. Impaired striatal cholinergic system in Dlx-CKO mice like earlier findings.
5. Affirms beam walking for preclinical screening in the absence of overt dystonia.

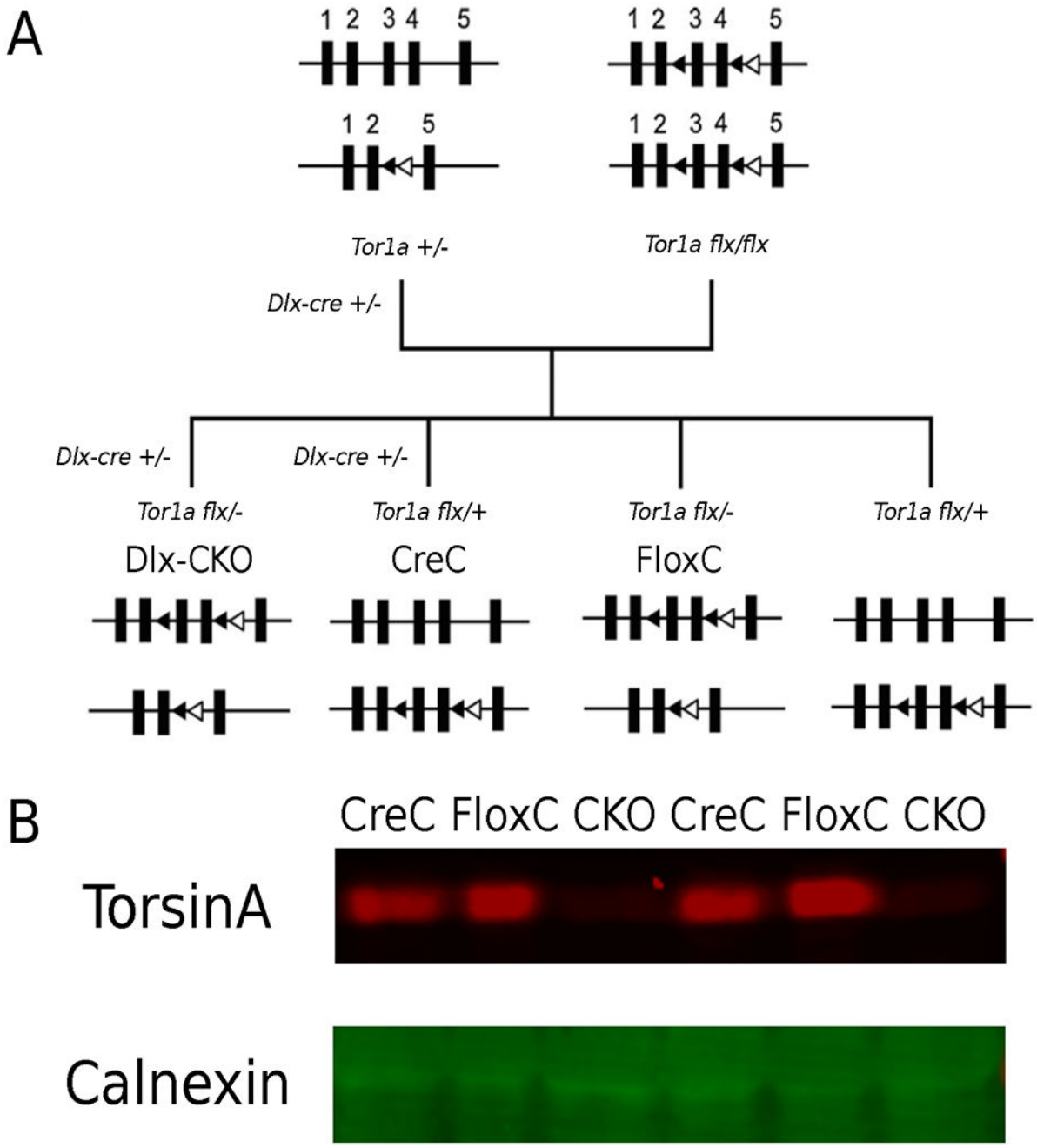

Fig. 1.

Breeding design and torsinA protein measurement. (A) Schematic diagram of the generation of Dlx-CKO mice. *Dlx-Cre*$^{+/-}$ *Tor1a*$^{+/-}$ crossed with *Tor1a*$^{flx/flx}$, with four possible offspring genotypes: *Dlx-Cre*$^{+/-}$ *Tor1a*$^{flx/-}$ (Dlx-CKO), *Dlx-Cre*$^{+/-}$ *Tor1a*$^{flx/+}$ (CreC), *Tor1a*$^{flx/-}$ (FloxC), and *Tor1a*$^{flx/+}$ (WT- not used). (B) Western blot of CreC (lanes 1 and 4), FloxC (lanes 2 and 5), and Dlx-CKO (lanes 3 and 6) demonstrating successful striatal torsinA knockout at 4-month-old mice.

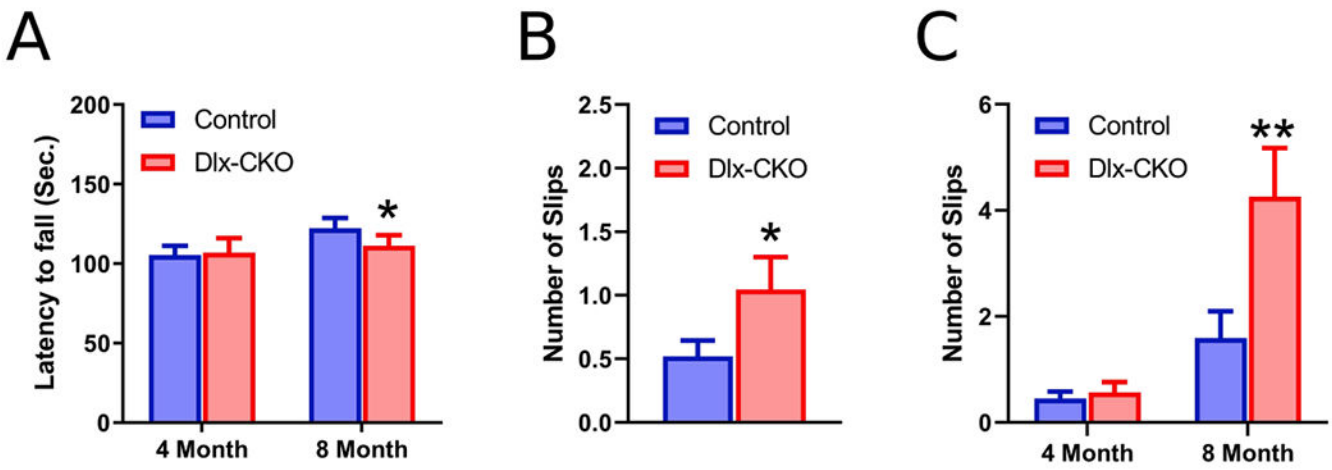

Fig. 2.

Paired 4-month and 8-month behavioral tests. (A) The accelerated rotarod test showed no difference between Dlx-CKO mice and control mice at 4 months, but latency to fall was significantly decreased in Dlx-CKO mice compared to control at 8 months. The 4-month cohort had 31 mice (14 CKO, 17 Control); 8-month cohort had 34 mice (17 CKO, 17 Control). (B) There were not enough slips among all experimental mice to determine the difference in slip number across all beams at 4 months. However, Dlx-CKO mice showed a significant increase in slip number across all beams at 8 months. (C) No difference was found between Dlx-CKO and control mouse slip number at 4 months on the small round and small square beams. However, at 8 months, Dlx-CKO mice showed a significantly increased number of slips. Bars represent mean ± standard error. *p<0.05, **p<0.01.

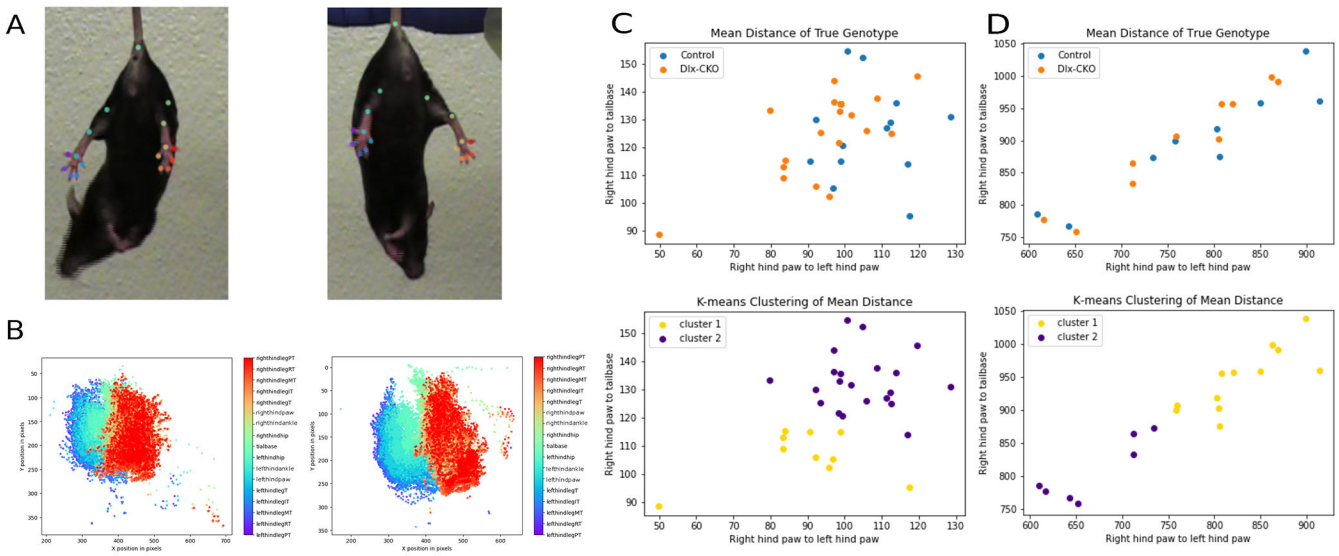

Fig. 3.

DeepLabCut application to determine motor phenotype. Application of body markers to major hindlimb joints (A - control left, Dlx-CKO right) and corresponding trajectory maps of markers throughout the video (B - control left, Dlx-CKO right). (C) 4-month and (D) 8-month K-means cluster analysis (bottom) and true genotypes of animals (top) plotted according to average relative distance in pixels between right hind paw vs. left hind paw (x-axis) and average relative distance in pixels between right hind paw and tail-base (y-axis). 52% agreement at 4 months and 53% agreement at 8 months were observed. 4-month cohort had 31 mice (14 CKO, 17 Control); 8-month cohort had 34 mice (17 CKO, 17 Control).

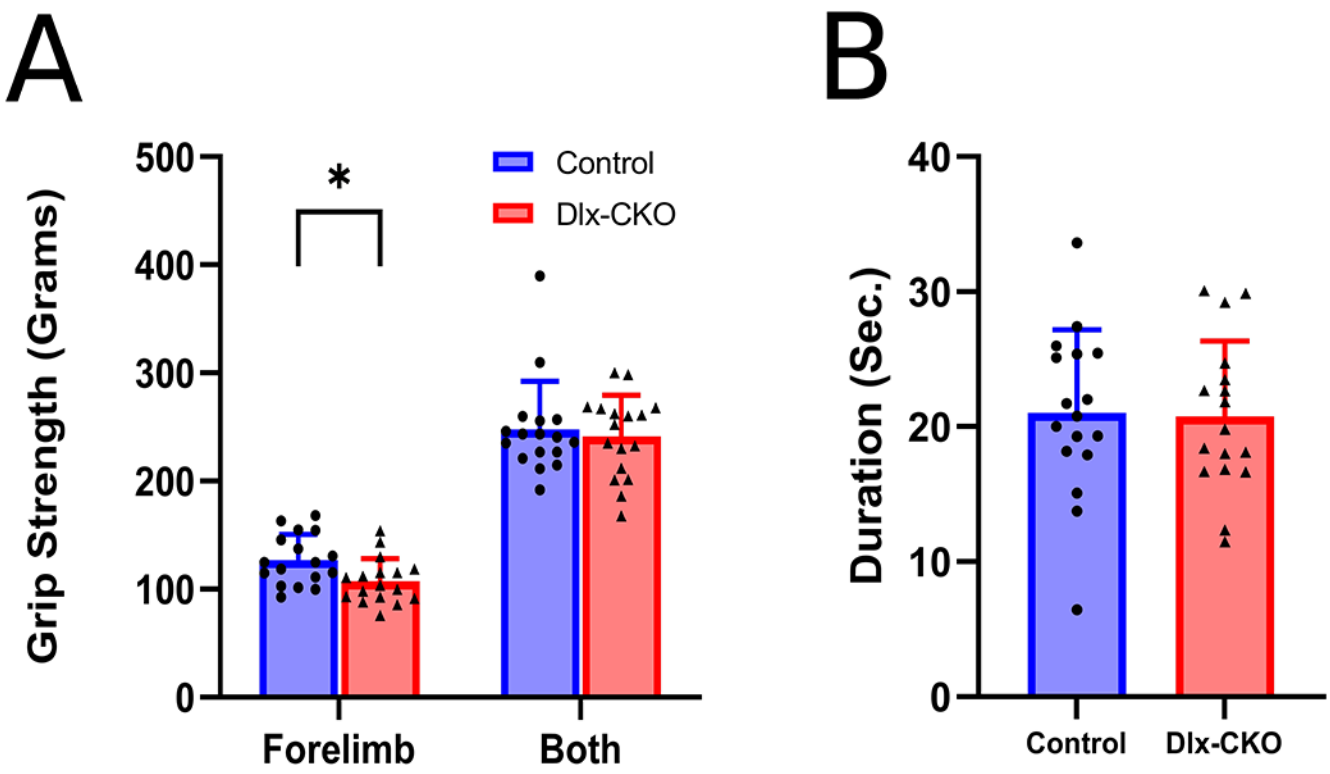

Fig. 4.

Grip Strength and Tail Suspension at 8 months - 34 mice (17 CKO, 17 Control). (A) No difference was found between the control and Dlx-CKO total grip strength; however, Dlx-CKO mice were found to have significantly reduced forelimb grip strength. (B) Duration of abnormal postures was scored through tail suspension recordings by two investigators blinded to genotype. No significant difference between Dlx-CKO mice and the control was observed. Bars represent mean ± standard error. *p<0.05.

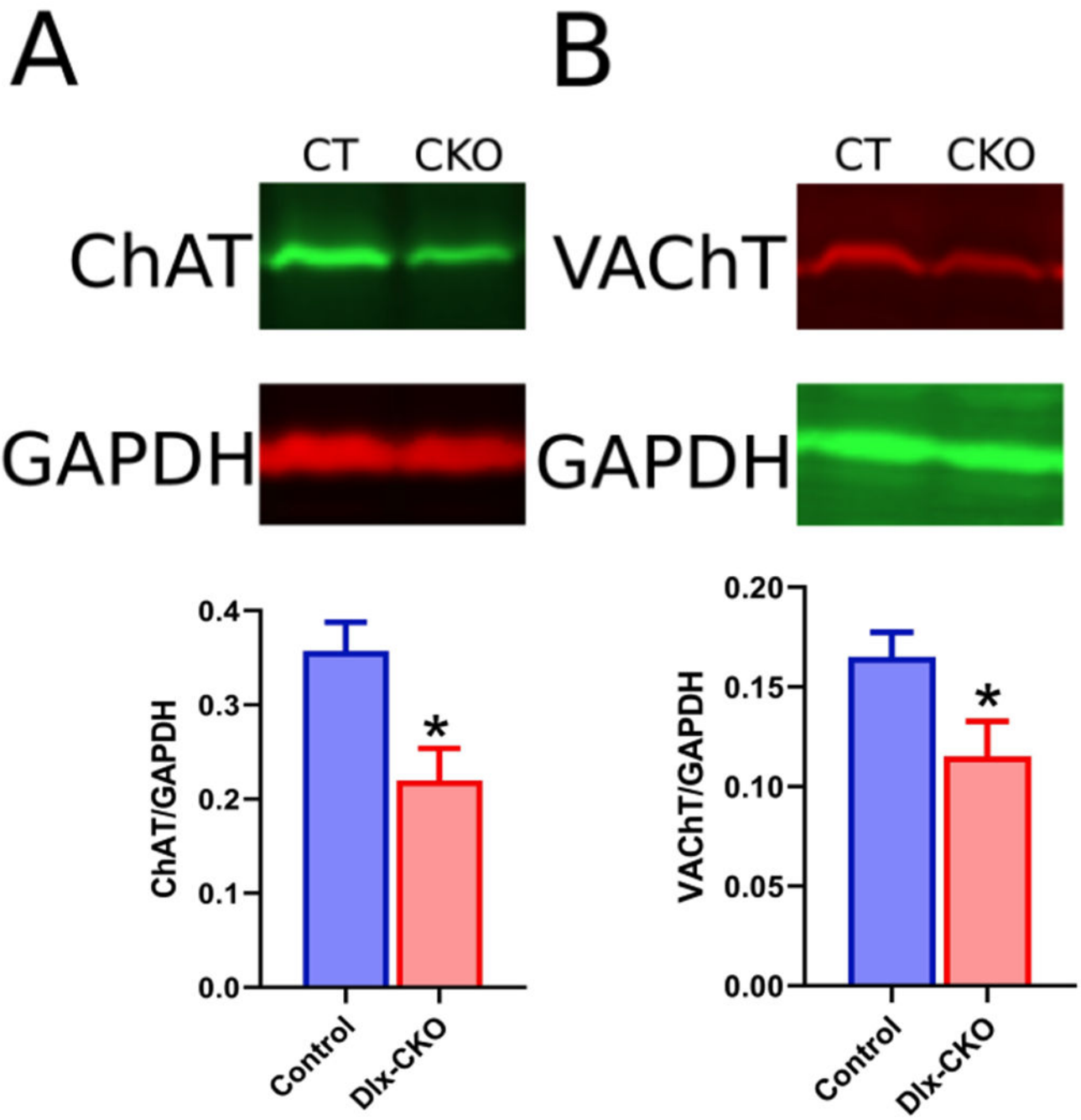

Fig. 5.

Representative images of Western blots of ChAT and VAChT and GAPDH controls. The quantified protein bands were standardized to GAPDH intensity. Significant reductions in ChAT (A) and VAChT(B) protein levels were found in Dlx-CKO 4-month-old mice. Bars represent mean ± standard error. *p<0.05.

Table 1.

Open field test of Dlx-CKO mice

Open Field Parameter	Control	Dlx-CKO	*p* value
Total Distance (cm)	2117.11±232.36	2805.85±309.72	0.0493*
Horizonal Activity	4513.31±361.86	504.33±407.73	0.3276
Number of Movements	246.33±18.63	268.49±20.53	0.3844
Movement Time (s)	227.21±21.65	292.17±27.86	0.0427*
Rest Time (s)	1569.53±28.59	1493.85±27.41	0.0401*
Vertical Activity	219.89±35.29	217.34±36.07	0.9563
Number of Vertical Movements	87.76±12.48	91.81±13.50	0.8111
Vertical Time (s)	79.826±13.86	71.22±12.59	0.6163
Sterotypy Counts	2235.58±210.64	2500.30±239.26	0.3667
Number of Sterotypy	240.58±8.92	245.45±9.17	0.6815
Sterotypy Time (s)	265.77±20.05	269.50±19.36	0.8937
Clockwise Revolutions	6.65±1.27	8.86±1.63	0.2367
Counterclockwise Revolutions	7.44±1.02	9.13±1.20	0.2288
Center Distance (cm)	507.48±97.37	704.39±137.61	0.1908
Center Time (s)	185.53±31.76	239.56±44.10	0.2635
Rearing Activity	218.66±35.03	216.82±35.90	0.9683
Number of Rearing Movements	87.86±12.50	91.89±13.52	0.8120
Rearing time (s)	79.62±13.81	71.08±12.56	0.6179